
CRS4

Centre for Advanced Studies,
Research and Development in Sardinia
Uta - (CA)

**Numerical simulations on the TEFLU sodium jet experiment
using the CFD code Karalis**

Date: November 7th 2000

by:

I. Di Piazza and M. Mulas
Fluid Dynamics and Combustion Area

abstract

The TEFLU experiments were performed at the Karlsruhe Forschungszentrum in order to investigate the behaviour of a low-Prandtl number jet under various flow conditions, from forced flow to purely buoyant. Here, numerical simulations are presented and results compared with the experimental data. The computations are made within the Benchmark Working Group activities in order to test the capabilities of CFD codes to simulate Heavy Liquid Metal flows with heat transfer. The simulations are performed with the CFD code **Karalis**.

Karalis is a parallel MPI, Finite-Volume, multiblock CFD code which solves the fully compressible Euler and Navier-Stokes equations where all couplings between dynamics and thermodynamics are allowed. This is the most general mathematical model for all fluid flows.

The code solves the coupled system of continuity, momentum and full energy equation for the velocity components, pressure and temperature. Once u , v , w , p and T are updated, arbitrary thermodynamics is supplied. A 5-stage Runge-Kutta explicit time-marching method is used to accelerate the convergence to steady state. This formulation, typical of aerodynamic flows, shows an excellent efficiency even for incompressible flows as well as for flows of incompressible fluids (typically buoyancy flows), once equipped with a preconditioner.

Karalis implements two among the most popular turbulence models, namely the one-equation model by Spalart and Allmaras and the two-equation model by Wilcox, the $\kappa - \omega$ model, which allow a good compromise between accuracy, robustness and stability of turbulent calculations.

For the simulations, the one-equation model of Spalart and Almaras was used for the turbulent calculations.

Contents

1	The experimental data	2
1.1	Description of the experimental conditions	2
1.2	The experimental results	4
2	The numerical simulations	6
2.1	Methods and models	6
2.2	Preliminary calculations	8
2.3	Benchmark calculations	9
3	Conclusions	12
4	References	13

1 The experimental data

1.1 Description of the experimental conditions

The TEFLU experiments [1] were performed at the Karlsruhe Forschungszentrum in order to assess the behaviour of a liquid metal jet in the presence of mixed (buoyant-forced) conditions. This is a topic of great interest for the safety-related removal of the decaying heat from a liquid metal fast breeder nuclear reactor. Many experiments were performed in the past using non liquid metal working fluids (see for example [2]), and results transferred to sodium via fluid dynamics similarity. The vertical axisymmetric jet chosen for the study was reported extensively in the literature, the first measurements having been made in air in the Wartime Report by Corrsin [3]. A comprehensive review of mixed forced-buoyant jet experiments is given by Chen and Rodi [4].

The experiments on the TEFLU apparatus are one of the few studies in which sodium was used. The kinematic viscosity of sodium ν is of a similar order of magnitude to that of water but the Prandtl number is three orders of magnitude lower and this gives a far greater significance to molecular diffusion in the energy equation. The high thermal conductivity will therefore cause temperature fluctuations to be damped out more rapidly than in ordinary fluids.

The test section consists essentially of a vertical pipe of 110 mm inner diameter and an axially movable jet block. The jet block contains 158 holes of diameter $d=7.2$ mm located on a triangular pitch of 8.2 mm. The temperature of the co-flow in the pipe is 573K. A sodium jet, heated to as much as 75 K above the co-flow temperature, is injected separately into the central hole of the jet block, which also has a diameter of $d=7.2$ mm. The uppermost 170 mm of the central pipe is also of 7.2 mm internal diameter and so the jet exit conditions correspond to a fully developed turbulent velocity profile at a uniform temperature.

A schematic representation of the experimental conditions is given in fig. 1 (see ref. [1] for a detailed representation of the TEFLU apparatus).

Measurements of mean velocity, mean temperature and temperature fluctuations are performed using a miniature permanent-magnet flowmeter probe, whose measuring principle is based on electromagnetic induction in liquid metals. Mean velocity profiles are revealed in sections $x/d = 6, 12, 20, 40$; while mean temperatures and fluctuations are measured in sections $x/d = 5, 11, 19, 39$ (distance from the jet block).

The following dimensionless numbers are chosen to describe the experimental conditions:

$$Re_{cf} = \frac{u_{cf} D}{\nu} \quad \text{co-flow Reynolds number}$$

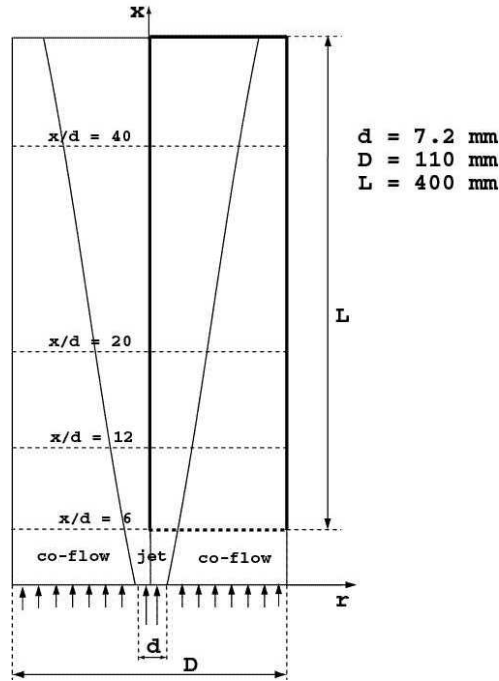


Figure 1: Schematic representation of the experimental conditions

$$Re_j = \frac{u_j d}{\nu} \quad \text{jet Reynolds number}$$

$$Fr_j = \frac{\rho(u_j^2 - u_{cf}^2)}{g(\rho_{cf} - \rho_j)d} \approx \frac{u_j^2 - u_{cf}^2}{g\beta(T_j - T_{cf})d} \quad \text{densimetric Froude number}$$

The densimetric Froude number represents the squared ratio of inertia to gravity forces, and can be regarded as the inverse of the Richardson number of the differential motion between the jet and the co-flow $Ri_{j-cf} = 1/Fr_j = Gr_{j-cf}/Re_{j-cf}^2$.

The physical properties of the liquid sodium vary slightly (less than 1%) in the temperature range of interest; thus, they can be evaluated at the reference co-flow temperature of 573K, and are provided in Table 1.

The experiments performed are summarised in Table 2, the dimensionless parameters being calculated on the basis of the physical properties in Table 1. In the following, for comparison purposes, only the case A will be addressed. Incidentally, the jet Reynolds number in Table 1 are far sufficient to ensure fully turbulent conditions, being the fluid motion dominated by shear, and by its inviscid instability mechanisms.

Property	symbol	value(SI units)
dynamic viscosity	μ	$3.446 \cdot 10^{-4}$
density	ρ	879.99
specific heat	c_p	1304.5
thermal conductivity	λ	76.58
thermal expansion coefficient	β	$2.975 \cdot 10^{-4}$
Prandtl number	Pr	$5.87 \cdot 10^{-3}$
kinematic viscosity	ν	$3.916 \cdot 10^{-7}$

Table 1: Physical properties of the liquid sodium at a reference temperature $T = 573K$

Case	Condition	u_{cf}	T_{cf}	Re_{cf}	u_j	T_j	Re_j	Fr_j	\dot{m}_{tot}
A	Forced jet	0.05	573	$1.4 \cdot 10^4$	0.55	603	$1.01 \cdot 10^4$	521	0.436
B	Buoyant jet	0.1	573	$2.8 \cdot 10^4$	0.43	598	$7.9 \cdot 10^3$	365	0.848
C	Plume	0.1	573	$2.8 \cdot 10^4$	0.27	648	$4.96 \cdot 10^3$	43.1	0.842

Table 2: Experimental conditions (SI units)

1.2 The experimental results

Experimental data of mean velocity and mean temperature in the various sections are shown in figs. 2 and 3 for the case A in Table 2.

Values at $x/d = 6$ were smoothed because they are provided as inlet profiles in the computations. It should be noticed that no measurements are available from $r = 40$ to the wall; therefore, the "tail" of the velocity data is somehow imposed to satisfy the global mass conservation:

$$\dot{m}_{tot} = 2\rho \int_0^D v \pi r dr \quad (1)$$

Nevertheless, data in section $x/d = 6$ seems more accurate and regular. On the contrary, the other experimental curves (especially $x/d = 12$) are affected by a high noise, and thus any comparison with numerical results must be considered just as qualitative. In addition, the velocity data points do not seem to satisfy the integral conservation law (1), keeping into account that the curves must be monotone. If an additional point is assigned ($x = 55.mm$, $v = 0.025$) to the series, and the data are interpolated by a 5th degree polinomial root mean square method , the

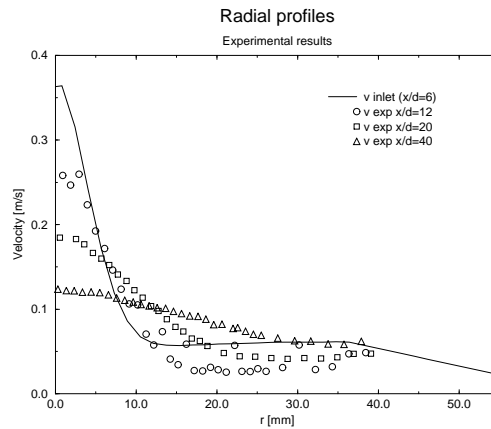


Figure 2: Experimental velocity profiles

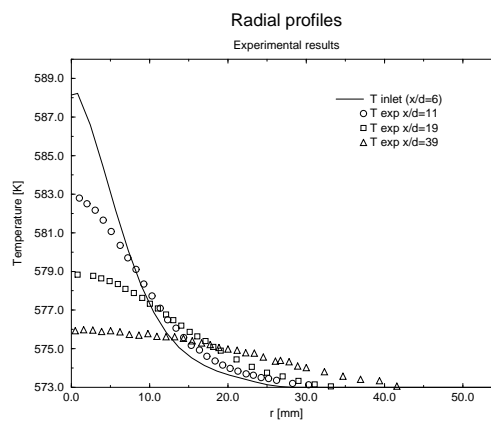


Figure 3: Experimental temperature profiles

integral (1) takes the values of 0.336, 0.386, 0.470 in sections $x/d = 12$, $x/d = 20$, $x/d = 40$ respectively; the error with respect to the value in Table 2 is of about 22% for the $x/d = 12$ data. The temperature data are also affected by an additional systematic error, showing unphysical values below the wall value of 573 K, although the low Prandtl number of sodium damps the irregularities with respect to the velocity profiles.

2 The numerical simulations

2.1 Methods and models

In this section numerical simulations are presented on the experimental conditions of the TEFLU apparatus and results compared with the experimental data. The computations are made within the Benchmark Working Group activities [5] in order to test the capabilities of CFD codes to simulate Heavy Liquid Metal flows with heat transfer. The computations are performed using the CFD code **Karalis**.

Karalis is a parallel MPI, Finite-Volume, multiblock CFD code which solves the fully compressible Euler and Navier-Stokes equations where all couplings between dynamics and thermodynamics are allowed. This is the most general mathematical model for all fluid flows.

The code solves the coupled system of continuity, momentum and full energy equation for the velocity components, pressure and temperature. Once u , v , w , p and T are updated, arbitrary thermodynamics is supplied. The second order Roe's upwind TVD scheme is used to compute convective fluxes through the Finite-Volume cell interfaces. A 5-stage Runge-Kutta explicit time-marching method is used to accelerate the convergence to steady state. This formulation, typical of aerodynamic flows, shows an excellent efficiency even for incompressible flows as well as for flows of incompressible fluids, once equipped with a preconditioner. Merkle's preconditioner was chosen because it can be easily formulated for arbitrary equations of state given as a functional relation of two independent thermodynamic variables. A more detailed description of the code algorithms and methods can be found in [6].

Although the buoyancy effects are probably negligible in the case A of Table 2, under consideration here, buoyant forces were taken into account in the simulations. The fluid is practically incompressible, but the flow is solved by the general compressible algorithm, letting the density to vary as a function of temperature and pressure by the general equation of state $\rho = \rho(p, T) = \rho_0 \exp[-\beta (T - T_0)]$, being the pressure dependence certainly negligible. The source term in the momentum equation is expressed as $(\rho - \rho_0)g$ (gravity direction), with the reference hydrostatic pressure gradient separated from the total pressure gradient and included in the source term:

$$-\nabla p + \rho \vec{g} \equiv -\nabla(p - p_0) + (\rho - \rho_0)\vec{g} \equiv -\nabla p' + (\rho - \rho_0)\vec{g}$$

The turbulence model used for the simulations is the one-equation model by Spalart & Allmaras [7]. It represents a simpler alternative, and more accurate also, to the widely used $\kappa - \epsilon$ model with wall functions. The additional equation of the model is written for a modified turbulent viscosity with a source term containing basically the strain rate tensor module approximated by the vorticity. The basic equation and

the expressions of the constants and of the wall functions are summarized in the following:

$$\mu_t = \rho \tilde{\nu} f_{v1}$$

$$\frac{D\tilde{\nu}}{Dt} = C_{b1} \tilde{\Omega} \tilde{\nu} + \frac{1}{\sigma} \frac{\partial}{\partial x_i} \left[(\nu + \tilde{\nu}) \frac{\partial \tilde{\nu}}{\partial x_i} \right] + \frac{C_{b2}}{\sigma} \frac{\partial \tilde{\nu}}{\partial x_k} \frac{\partial \tilde{\nu}}{\partial x_k} - C_{w1} f_w \left[\frac{\tilde{\nu}}{d} \right]^2$$

$$f_{v1} = \frac{\chi^3}{\chi^3 + c_{v1}^3}$$

$$\chi = \frac{\tilde{\nu}}{\nu}$$

$$\tilde{\Omega} = \Omega + \frac{\tilde{\nu}}{\kappa^2 d^2} f_{v2}$$

$$f_{v2} = 1 - \frac{\chi}{1 + \chi f_{v1}}$$

$$f_w = g \left(\frac{1 + c_{w3}^6}{g^6 + c_{w3}^6} \right)^{1/6}$$

$$g = r + c_{w2}(r^6 - r)$$

$$r = \frac{\tilde{\nu}}{\tilde{\Omega} \kappa^2 d^2}$$

$$c_{w1} = \frac{C_{b1}}{\kappa} + \frac{1 + C_{b2}}{\sigma}$$

C_{b1}	C_{b2}	σ	κ	C_{w3}	C_{w2}	C_{v1}
0.135	0.622	2/3	0.41	2	0.3	7.1

where Ω represents again the absolute value of vorticity, and d the distance from the closest solid boundary. The $\kappa - \omega$ model by Wilcox [8] hasn't been yet fully tested in conjunction with Merkle's preconditioning and low Prandtl number fluids, and thus it hasn't been used here.

2.2 Preliminary calculations

As a first step to the calculations proposed by the benchmark promoters, the entire domain sketched in fig. 1 was simulated by imposing inlet step profiles for velocity and temperature (section $x/d = 0$), taking the values for jet and co-flow according to case A in Table 2. Different inlet boundary conditions (both Dirichlet and Neumann) were tried in order to confirm the experimental curves at $x/d = 6$. The best agreement was obtained using a value of $7.5 \cdot 10^{-5}$ for the modified turbulent kinematic viscosity $\tilde{\nu}$ in the Spalart & Allmaras turbulence model. The same order of magnitude can also be derived from the air experimental data of Corrsin[3] by similarity consideration. A constant temperature of 573K was imposed at the wall. The turbulent Prandtl number Pr_t was fixed to 1.3.

No significant variation of the results was noticed using computational grids of 34×140 and 68×140 (both uniformly spaced), being the solutions practically grid-independent.

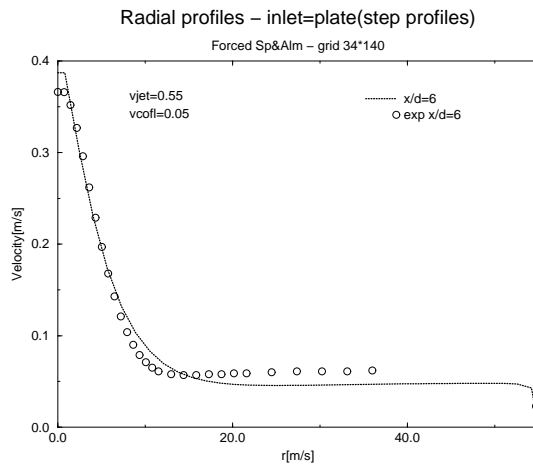


Figure 4: Comparison between numerical velocity profiles and experimental data in section $x/d = 6$

A comparison of the numerical solution and the experimental data in the section $x/d=6$ is shown in figs. 4 and 5. The agreement for velocity is rather good, while there is an underestimation in temperatures, suggesting that a higher turbulence Prandtl number could be required for liquid metals.

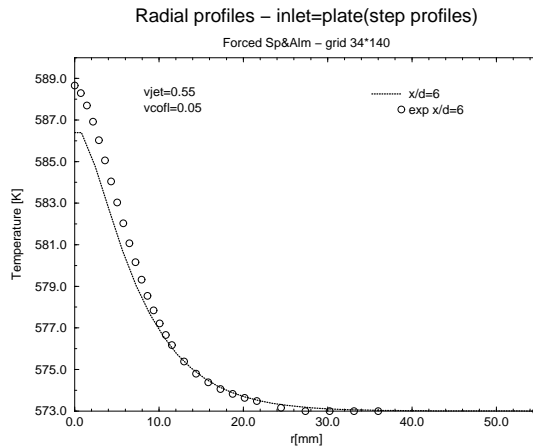


Figure 5: Comparison between numerical temperature profiles and experimental data in section $x/d = 6$

2.3 Benchmark calculations

With reference to fig. 1, the computational domain was restricted from $x/d = 6$ (inlet) to $x/d = 61.5$ (outlet), following the prescriptions of the benchmark promoters. The inlet boundary conditions were the regularized experimental data of velocity and temperature in section $x/d = 6$. For turbulence viscosity, the constant value of $7.5 \cdot 10^{-5}$ was imposed at the inlet, according to the preliminar calculations documented in 2.2. A constant temperature of 573K was imposed at the wall, while the turbulent Prandtl number Pr_t was fixed to 1.3.

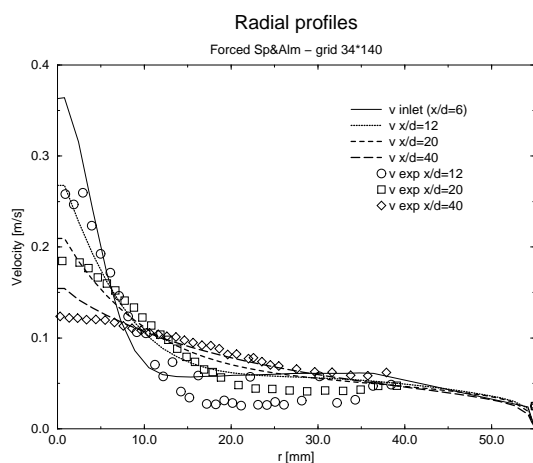


Figure 6: Comparison between numerical velocity profiles and experimental data

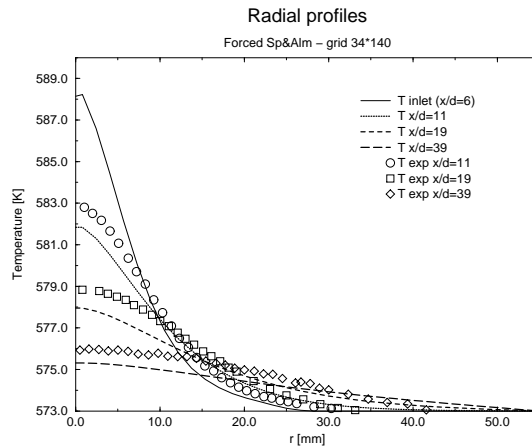


Figure 7: Comparison between numerical temperature profiles and experimental data

The comparison between experimental and numerical velocity radial profiles at the various sections is shown in fig. 6. The great dispersion of data relative to section $x/d = 12$ renders any quantitative comparison in this section very difficult. Nevertheless, experimental velocities below 0.04 are surely unphysical, being the co-flow velocity value 0.05. For the other sections ($x/d = 20, 40$), the most relevant fact is an overestimation in the "jet" region ($r < 10$ mm), due obviously to an underprediction of turbulent viscosity by the turbulence model. In any case, it should be stressed that the qualitative distribution of turbulence viscosity in the domain seems to be very reasonable, giving maxima where the vorticity is higher, being the turbulence production dominated by shear.

By the opposite, a global underestimation of temperatures can be clearly observed in fig. 7. As mentioned earlier, this fact could be due to higher values of Pr_t required by liquid sodium at these Reynolds numbers.

The axial profiles in figs. 8 and 9 simply confirm the previous remarks.

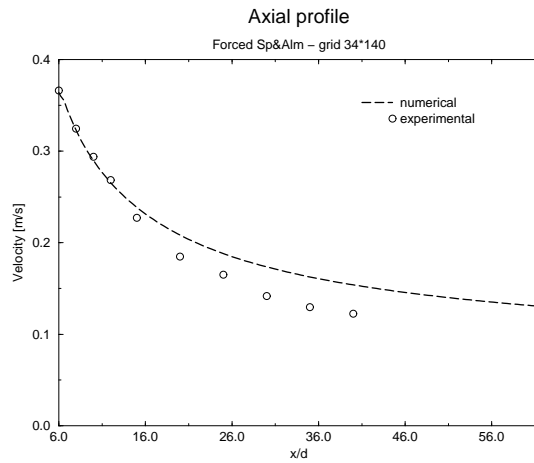


Figure 8: Comparison between numerical velocity profiles and experimental data

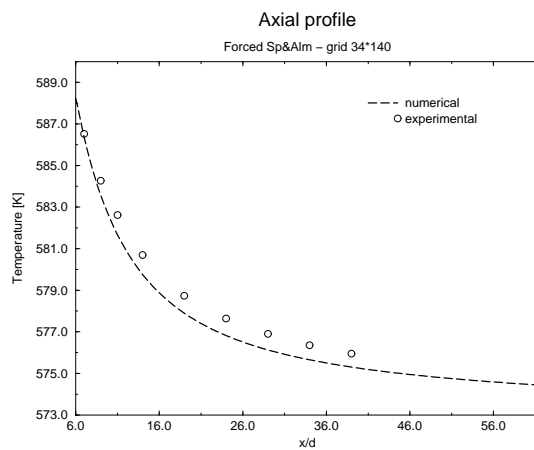


Figure 9: Comparison between numerical temperature profiles and experimental data

3 Conclusions

Numerical simulations were performed on the experimental data of the TEFLU apparatus [1] within the benchmark activity of the Benchmark Working Group [5]. The CFD code **Karalis** [6] with the one-equation turbulence model by Spalart & Allmaras [7] was used for the simulations. The experimental data exhibit a great dispersion, making the comparison with numerical results difficult. In particular data in section $x/d = 12$ seems to violate the global mass conservation. Preliminary calculations showed that taking the inlet section at $x/d = 0$ with an inlet value of $7.5 \cdot 10^{-5}$ for the turbulence viscosity and step velocity and temperature inlet profiles, the experimental data in section $x/d = 6$ were well reproduced. Nevertheless, following the benchmark promoters suggestions, the inlet section was placed at $x/d = 6$, giving the regularized experimental profiles as inlet profiles for velocity and temperature. The calculations showed a global overestimation of velocity in the "jet" axial region, and an underestimation of temperature. The underprediction of the turbulent viscosity by the turbulence model is the main reason for the higher velocities computed, while the underprediction in temperature is probably due to the higher turbulent Prandtl number required for liquid metals under this flow conditions.

4 References

- [1] Knebel J. U. *et al* : *Experimental investigation of a confined heated sodium jet in a co-flow* J. of Fluid Mechanics, vol.368, 1998.
- [2] Rust K. *et al* : *Summary report of steady state NEPTUN investigations into passive decay heat removal by natural convection* , FZKA Report 5665, 1995.
- [3] Corrsin S. : *Investigation of flow in an axially symmetric heated jet of air* , NACA Wartime Report W-94, 1943.
- [4] Chen K. & Rodi W. : *Turbulent Buoyant Jets - A Review of Experimental Data* , HMT vol.4, Pergamon Press, 1980.
- [5] Buono S. : *Minutes of the First meeting of the Benchmark Working Group on Heavy Liquid Metal thermal-hydraulics* , CERN Report, June 29-30, 1999, Geneva.
- [6] Mulas M. *et al* : *The CFD Code Karalis* , CRS4 Report, 2000.
- [7] Spalart & Almaras : *A one-equation turbulence model for aereodynamic flows* , La Recherche Aerospatiale, no.1, 1994.
- [8] Wilcox D.C. : *Reassessment of the scale-determining equation for advanced turbulence models* , AIAA J., vol.26, no.11, 1988.